Surface Modification of TiO₂ Nanoparticles with Phenyltrimethoxysilane in Dye-sensitized Solar Cells

Yong-June Chang,[a] Byung-Gon Kum,[†,a] Yoon-Cheol Park,[‡] Eui-Hyun Kong, and Hyun Myung Jang[*]

Department of Materials Science and Engineering, and Division of Advanced Materials Science, Pohang University of Science and Technology (POSTECH), Pohang 790-784, Korea. [*]E-mail: hmjang@postech.ac.kr
[†]Samsung Display Co. Ltd., Yongin 446-711, Korea
[‡]Research Institute of Industrial Science and Technology (RIST), Pohang 790-784, Korea

Phenyltrimethoxysilane (PTMS) was anchored onto the sensitized TiO₂ nanoparticles. This insulating molecular layer effectively inhibited the charge recombination at the interface of TiO₂/electrolyte in the dye–sensitized solar cells (DSCs) without sacrificing the dye-loading capacity of the nanocrystalline TiO₂. DSCs using PTMS-modified TiO₂ exhibited a short-circuit current (J_{SC}) of 15.9 mA/cm², an open-circuit voltage (V_{OC}) of 789 mV, and a fill factor (FF) of 68.2%, yielding an overall conversion efficiency (η) of 8.55% under 100 mW/cm² illumination. The resulting cell efficiency was improved by ~10% as compared with the reference cell.

Key Words : Dye-sensitized solar cells, Surface modification, TiO₂

Introduction

Dye–sensitized solar cells (DSCs) have attracted a great deal of attention because of their low–cost production and relatively high light–to–electric conversion efficiency. DSCs are composed of working electrodes (nanocrystalline TiO₂ film on fluorine–doped tin oxide), sensitizing dye, and Pt counter electrodes.[1,2] Thick TiO₂ nanoparticle film provides sufficient anchoring sites for dye molecules, which excite electrons by absorbing photons to produce electric current. This large surface, however, also promotes the back electron transfer at the solvent–exposed parts of the TiO₂, which is considered to be a main limitation on the cell efficiency.[3] Thus, much effort has been made in the surface modification of TiO₂ to reduce the degree of the interfacial charge recombination between the TiO₂ surface and the electrolyte.

A coadsorbent molecule such as hexadecylmalonic acid,[4] chenodeoxycholic acid,[5,6] 1–decyl phosphonic acid[7] or 3–phenyl–propionic acid[8] can be used to suppress the recombination. Coadsorbents, in general, prohibit the aggregation of dye molecules to increase the dye–loading capability or change the energy band structure at the interface of TiO₂/dye/electrolyte. Resultantly, the photocurrent density of the sensitized cells can be enhanced owing to the improved electron injection efficiency.[9-15] Alternatively, metal oxides such as Al₂O₃,[16-18] SiO₂,[18] ZrO₂,[18] and Nb₂O₅[19-21] can be coated on the TiO₂ surface to create a wider band-gap. Such oxide barrier layers effectively suppress charge recombination at the interface between the TiO₂ and the electrolyte, thereby improving the open circuit voltage. However, conformal coating of these barrier layers may be difficult to control. Moreover, metal-oxide-coating methods can reduce the surface area of TiO₂ and form an insulating barrier

between dye and TiO₂, which degrades the electron injection efficiency. Although both strategies for blocking recombination phenomena improve the cell efficiency, their usages may be limited to specific cases and sometimes worsen the light harvest of a given cell.

Here, we introduce phenyltrimethoxysilane (PTMS) as an insulating molecular layer in the photoanode of DSCs. Through the simple post-treatment of the sensitized TiO₂ electrode, PTMS molecules have been anchored on the uncovered TiO₂ surface without detaching the dye molecules, thereby reducing the interfacial reaction that affects the charge recombination. To our knowledge, this is the first demonstration in the DSCs with nanocrytalline TiO₂ of grafting a silane-based molecule.

Experimental Section

Preparation of the Photoelectrodes. For the present experiment, two different photoelectrodes were used: one was the PTMS–treated DSC and the other for the reference cell that had no surface modification. A fluorine-doped SnO₂ (FTO) glass substrate was pre-cleaned by isopropyl alcohol, deionized (D.I.) water, and acetone. A 15-µm–thick nanocrystalline TiO₂ film (T20/SP, Solaronix) and a 5-µm–thick TiO₂ scattering particle film (CCIC) were deposited on the substrate using a screen printer. Curing in a furnace followed a temperature profile: (i) at 325 °C for 5 min, (ii) at 375 °C for 5 min, (iii) at 450 °C for 15 min, and (iv) at 500 °C for 15 min. The electrode soaking in 40 mM aqueous TiCl₄ solution was stored in an oven at 70 °C for 30 min, then rinsed with D.I. water and ethanol to ensure good adhesion properties at the TiO₂/FTO interface. The TiCl₄-treated electrode was heated again at 500 °C for 30 min. The photoelectrode was immersed into the 0.5 mM N719 dye solution, and kept at room temperature for 24 h. For the PTMS modification of

---

Table 1. Photovoltaic properties of the DSCs with various PTMS treatment times

Treatment time (minutes)	V_{oc} (mV)	J_{sc} (mA/cm^2)	Fill factor (%)	Efficiency (%)
0	789±1	14.5±0.1	68.1±0.3	7.79±0.10
0.5	792±1	14.6±0.1	68.4±0.1	7.91±0.08
1.0	795±1	14.9±0.2	68.9±0.1	8.16±0.13
1.5	789±0	15.9±0.2	68.2±0.3	8.55±0.14
2.0	799±1	13.9±0.1	66.8±0.1	7.42±0.07
2.5	795±0	13.6±0.2	67.3±0.2	7.28±0.13

the nanocrystalline TiO$_2$ film, the dye-sensitized photo-electrode was dipped in the PTMS solution (0.8 g PTMS dissolved in 50 mL ethanol) with various dipping times: from 0 to 2.5 min. The treatment time-dependent photovoltaic properties are shown in Table 1. It was found that the current density increases with the PTMS-treatment time up to 1.5 min. However, beyond this time (1.5 min), the PTMS-treatment even deteriorated the cell efficiency. Consequently, we took 1.5 min as the optimum PTMS-treatment time for the dye-sensitized cells.

Cell Fabrication. The counter electrode was prepared by dripping a Pt solution (Platisol T, Solaronix) on the FTO substrate, which had been followed by the thermal treatment at 500 °C for 30 min. For the cell assembly, a hot-melt 60-ìm-thick Surlyn (Meltonix 1170-60, Solaronix) was used as a spacer between the photoelectrode and the counter electrode. The electrolyte (AN50, Solaronix) was injected through a hole which was then sealed.

Characterizations. ^{29}Si CP-MAS NMR spectra were recorded using a Brüker DSX 400M Hz instrument equipped with a 4 mm solid-state probe operating at 79.5 MHz for ^{29}Si nuclei. The spectra were collected using a magic angle spinning speed of 8 kHz. Diffuse reflectance spectra were measured by using a UV-VIS spectrometer (Perkin Elmer Lambda 750S) in order to obtain absorption spectra of the sensitized photoelectrodes. For the evaluation of the dye-loading capacity, the dye attached on the two distinct TiO$_2$ electrodes (with and without the PTMS treatment) were dissolved in a 3 mL 0.1 M NaOH solution of water and ethanol (50/50, v/v), and the absorption properties were compared with the 3 mL 0.03 mM N719 solution by using the UV-Vis spectrometer. Recombination resistance was investigated by employing electrochemical impedance spectroscopy (EIS) under air mass 1.5 1 sun illumination (AM 1.5, 100 mW/cm^2). EIS was conducted under various applied biases near the cell V_{oc} (850, 800, and 750 mV). I-V curves were obtained using a Keithley 2400 model as a source measurement unit. One sun of light (100 mW cm^{-2}) was simulated using an Oriel solar simulator. The light intensity was adjusted with a NREL-calibrated silicon standard cell. Photon-to-current conversion efficiency (IPCE) was measured as a function of wavelength from 400 to 800 nm at a low chopping frequency of 10 Hz (PV Measurements, Inc). A 75W Xenon lamp was used as a light source with a mono-chromator. Calibration was performed using a NIST-calibrated

photodiode (G425) as a reference.

Results and Discussions

^{29}Si CP-MAS NMR Analysis on the PTMS-modified TiO$_2$ Nanoparticles. As shown in Figure 1, PTMS molecules are anchored onto the sensitized TiO$_2$ surface. A blocking layer can be created by the condensation of hydroxide groups (OH-) formed at the TiO$_2$ surface with methoxy groups (-OCH$_3$) of PTMS. The PTMS-modified TiO$_2$ surface was analyzed by ^{29}Si MAS NMR. As shown in Figure 2, three characteristic peaks corresponding to T^1[Si(OMt)$_2$(OTi)$_1$R], T^2[Si(OMt)$_1$(OTi)$_2$R], T^3[Si(OMt)$_0$(OTi)$_3$R] were observed at −46, −57, −69 ppm, respectively, indicating the presence of PTMS on the TiO$_2$ nanoparticles.[22,23]

Influence of the PTMS Treatment on the Dye-loading Capacity. The amount of the adsorbed dye molecules can be
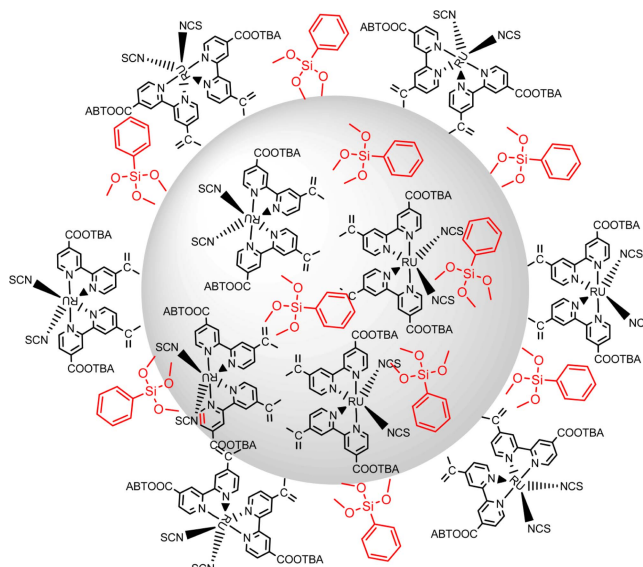

Figure 1. Grafting of phenyltrimethoxysilane (PTMS) on the TiO$_2$ nanoparticle surface by the condensation step.
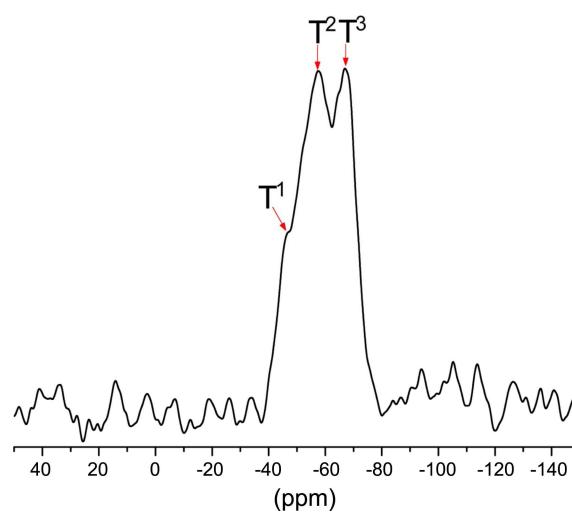

Figure 2. ^{29}Si MAS NMR spectrum of organo–silicone compounds anchored on the TiO$_2$ nanoparticle surface.

characterized by measuring the absorbance spectra of the sensitized working electrodes. However, it is difficult to directly obtain the absorbance values using a UV-Vis spectroscopy since a typical bi-layered photoelectrode has no transparency due to the presence of the light scattering layer. To deal with this problem, one can derive the absorbance from the diffuse reflectance of the sensitized photoelectrodes by using the following Kubelka-Munk equation.

$$F(R) = (1-R)^2/2R = k/s = Ac/s$$

(R: reflectance, k: absorption coefficient, s: scattering coefficient, c: concentration of the absorbing species, and A: absorbance.)

As shown in Figure 3(a), the absorbance value is scarcely affected by the PTMS treatment for a wide range of the wavelength. This implies that PTMS does not compete with the dye molecule in the chemisorption at the TiO₂ surface.

As a next step, dye molecules were detached from the two distinct TiO₂ electrodes (active area: 1.0 cm²) by using a 0.1 M NaOH solution. Then, their absorbance values were compared with the reference N719 solution (0.90×10^{-7} mol) for the quantitative evaluation of the dye-loading properties

(Figure 3(b)). Accordingly, two working electrodes showed almost identical loading capacities (1.22×10^{-7} mol/cm² for the PTMS electrode, and 1.24×10^{-7} mol/cm² for the reference), which is in good agreement with the previous result from the diffuse reflectance analysis. Therefore, it can be concluded that the PTMS molecules graft only on the uncovered TiO₂ surface where the dye molecules do not chemically adsorb.

EIS Measurement. Electrochemical impedance spectroscopy (EIS) study was carried out in order to study electron transport kinetics in the DSCs.[24-26] The effective lifetime of electrons (τ_{eff}) and the charge–transfer resistance (R_k) were estimated from the EIS measurement. EIS was conducted under various applied biases near the cell V_{oc} (850, 800, and 750 mV) with 100 mW/cm² illumination. It is known that the second semicircle in the Nyquist plot is related to R_k between the TiO₂ and the electrolyte. τ_{eff} is given by the following relation.[26]

$$\tau_{eff} = 1/\omega_{max}$$
(ω_{max} : the peak frequency of an arc in a Nyquist plot)

Figure 4 shows that R_k and τ_{eff} for the PTMS−modified cell are 23.98 Ω/0.189 s⁻¹ at 750 mV, 13.45 Ω/0.119 s⁻¹ at 800 mV, and 8.12 Ω/0.093 s⁻¹ at 850 mV, respectively; in comparison, those values are 16.6 Ω/0.118 s⁻¹ at 750 mV, 8.97 Ω/0.074 s⁻¹ at 800 mV, and 6.65 Ω/0.059 s⁻¹ at 850 mV for the reference cell. It is clear that both the recombination resistance and the effective electron life time increase noticeably by the PTMS treatment. We attribute this result to the
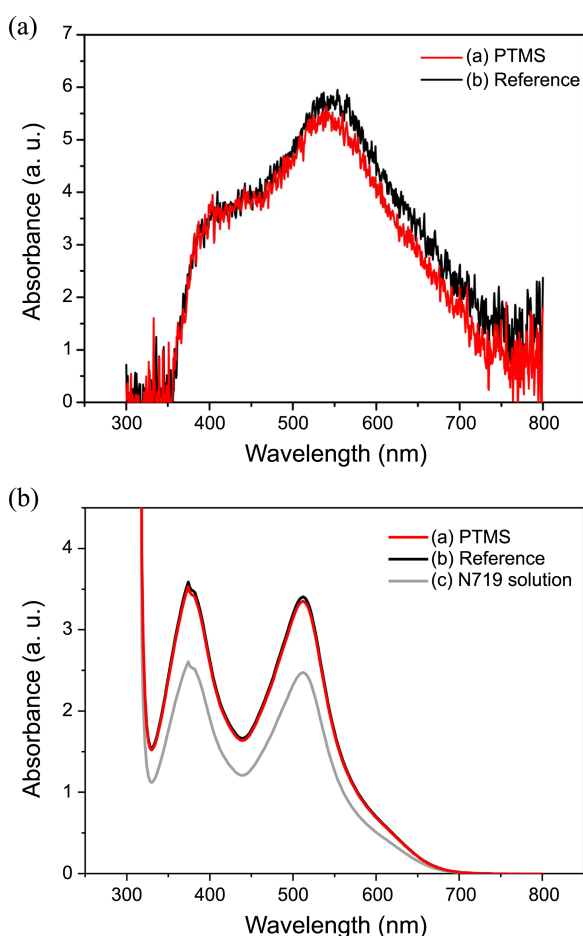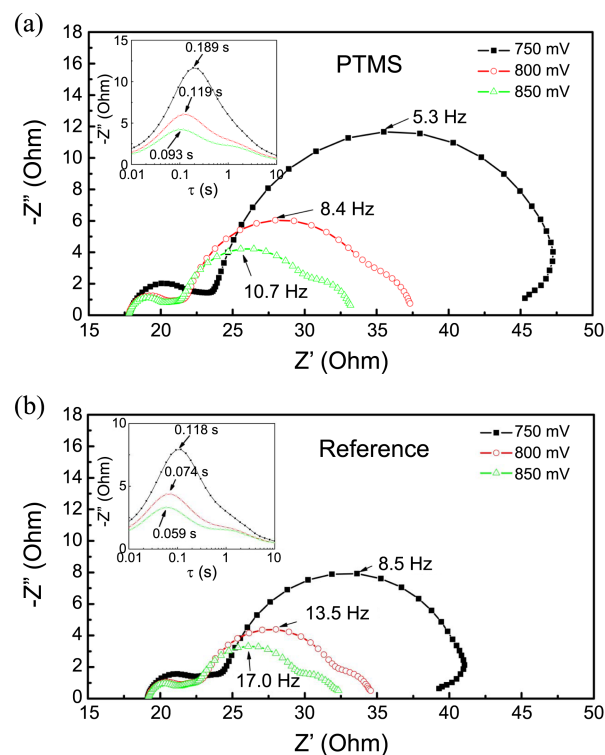

(a)

(b)

Figure 3. Absorbance of the sensitized TiO₂ electrodes (with and without the PTMS treatment) derived from the diffuse reflectance by using Kubelka-Munk equation (a). Absorbance of N719 dye molecules detached from the two distinct TiO₂ electrodes in comparison with the reference 0.03 mM N719 dye solution (b).

(a)

(b)

Figure 4. Impedance analysis for the charge–transfer resistance and the effective electron lifetime (insect figure) of the DSCs with (a) and without (b) the PTMS treatment.
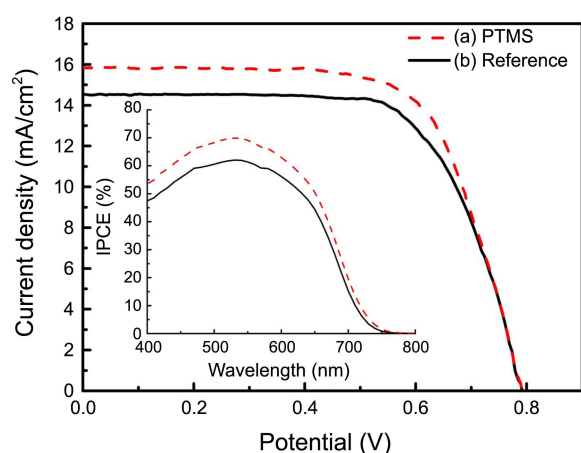
418   *Bull. Korean Chem. Soc.* **2014**, Vol. 35, No. 2

Yong-June Chang *et al.*

Figure 5. IV curves of the DSCs and incident–photon–to–current conversion efficiencies with (a) and without (b) the PTMS treatment.

Table 2. Photovoltaic properties of the DSCs with and without the PTMS treatment

Sample	V_{oc} (mV)	J_{sc} (mA/cm^2)	Fill factor (%)	Efficiency (%)
Reference	789±1	14.5±0.1	68.1±0.3	7.79±0.10
PTMS	789±0	15.9±0.2	68.2±0.3	8.55±0.14

adsorbed PTMS molecules, which functioned as a recombination blocking layer between the TiO$_2$ surface and the electrolyte.

Photovoltaic Properties. The surface modification effect is also reflected in the I–V curves (Figure 5). The photovoltaic parameters of the DSCs with and without the PTMS treatment are summarized in Table 2. Interestingly, the PTMS–treated device showed noticeable enhancement in J_{sc} and FF, resulting in higher overall conversion efficiency: 8.55% versus 7.79% for the reference cell. The incident–photon–to–current conversion efficiency (IPCE) shows more detailed information on the light harvest of the DSCs (inset of Figure 5). The overall IPCE values are increased after the surface modification with PTMS, which is in good agreement with the improved J_{sc} observed in the I–V curves.

In conclusion, PTMS, a silane–based molecule, was employed to modify the TiO$_2$ surface, and its influence on the DSCs was studied. It was confirmed that PTMS was successfully anchored on the TiO$_2$ nanoparticles as shown in the solid–state NMR analysis. ~10% increase in the overall efficiency was achieved after the PTMS treatment. EIS analysis suggests that the improvement in J_{sc} is caused by the effective suppression of the interfacial charge recombination between the TiO$_2$ surface and the electrolyte. Therefore, this observation may pave a way for use of silanol–based molecule as a promising surface modifier in DSCs.

References

1. Nazeeruddin, M. K.; De Angelis, F.; Fantacci, S.; Selloni, A.; Viscardi, G.; Liska, P.; Ito, S.; Takeru, B.; Grätzel, M. *J. Am. Chem. Soc.* **2005**, *127*, 16835-16847.
2. Grätzel, M. *Inorg. Chem.* **2005**, *44*, 6841-6851.
3. Lin, Z. Q.; Wang, J. *Chem. Mater.* **2010**, *22*, 579-584.
4. Wang, P.; Zakeeruddin, S. M.; Comte, P.; Charvet, R.; Humphry-Baker, R.; Grätzel, M. *J. Phys. Chem. B* **2003**, *107*, 14336-14341.
5. Ito, S.; Miura, H.; Uchida, S.; Takata, M.; Sumioka, K.; Liska, P.; Comte, P.; Pechy, P.; Grätzel, M. *Chem. Comm.* **2008**, 5194-5196.
6. Morandeira, A.; Lopez-Duarte, I.; O'Regan, B.; Martinez-Diaz, M. V.; Forneli, A.; Palomares, E.; Torres, T.; Durrant, J. R. *J. Mater. Chem.* **2009**, *19*, 5016-5026.
7. Wang, P.; Zakeeruddin, S. M.; Humphry-Baker, R.; Moser, J. E.; Grätzel, M. *Adv. Mater.* **2003**, *15*, 2101-2104.
8. Wang, P.; Zakeeruddin, S. M.; Humphry-Baker, R.; Grätzel, M. *Chem. Mater.* **2004**, *16*, 2694-2696.
9. Burke, A.; Schmidt-Mende, L.; Ito, S.; Gratzel, M. *Chem. Commun.* **2007**, 234-236.
10. Hara, K.; Dan-Oh, Y.; Kasada, C.; Ohga, Y.; Shinpo, A.; Suga, S.; Sayama, K.; Arakawa, H. *Langmuir* **2004**, *20*, 4205-4210.
11. Nazeeruddin, M. K.; Humphry-Baker, R.; Grätzel, M.; Wohrle, D.; Schnurpfeil, G.; Schneider, G.; Hirth, A.; Trombach, N. *J. Porphyr. Phthalocya.* **1999**, *3*, 230-237.
12. Reddy, P. Y.; Giribabu, L.; Lyness, C.; Snaith, H. J.; Vijaykumar, C.; Chandrasekharam, M.; Lakshmikantam, M.; Yum, J. H.; Kalyanasundaram, K.; Graetzel, M.; Nazeeruddin, M. K. *Angew. Chem. Int. Ed.* **2007**, *46*, 373-376.
13. Sayama, K.; Tsukagoshi, S.; Mori, T.; Hara, K.; Ohga, Y.; Shinpou, A.; Abe, Y.; Suga, S.; Arakawa, H. *Sol. Energ. Mater. Sol. C* **2003**, *80*, 47-71.
14. Wang, Z. S.; Cui, Y.; Dan-Oh, Y.; Kasada, C.; Shinpo, A.; Hara, K. *J. Phys. Chem. C* **2007**, *111*, 7224-7230.
15. Yum, J. H.; Jang, S. R.; Humphry-Baker, R.; Grätzel, M.; Cid, J. J.; Torres, T.; Nazeeruddin, M. K. *Langmuir* **2008**, *24*, 5636-5640.
16. Wu, S. J.; Han, H. W.; Tai, Q. D.; Zhang, J.; Xu, S.; Zhou, C. H.; Yang, Y.; Hu, H.; Chen, B. L.; Zhao, X. Z. *J. Power Sources* **2008**, *182*, 119-123.
17. Zhang, X. T.; Sutanto, I.; Taguchi, T.; Meng, Q. B.; Rao, T. N.; Fujishima, A.; Watanabe, H.; Nakamori, T.; Uragami, M. *Sol. Energ. Mater. Sol. C* **2003**, *80*, 315-326.
18. Palomares, E.; Clifford, J. N.; Haque, S. A.; Lutz, T.; Durrant, J. R. *J. Am. Chem. Soc.* **2003**, *125*, 475-482.
19. Diamant, Y.; Chappel, S.; Chen, S. G.; Melamed, O.; Zaban, A. *Coord. Chem. Rev.* **2004**, *248*, 1271-1276.
20. Chen, S. G.; Chappel, S.; Diamant, Y.; Zaban, A. *Chem. Mater.* **2001**, *13*, 4629-4634.
21. Zaban, A.; Chen, S. G.; Chappel, S.; Gregg, B. A. *Chem. Commun.* **2000**, 2231-2232.
22. Glaser, R. H.; Wilkes, G. L.; Bronnimann, C. E. *J. Non-Cryst. Solids* **1989**, *113*, 73-87.
23. Cerneaux, S.; Zakeeruddin, S.; Pringle, J.; Cheng, Y. B.; Grätzel, M.; Spiccia, L. *Adv. Funct. Mater.* **2007**, *17*, 3200-3206.
24. Willig, F. *J. Phys. Chem. B* **2003**, *107*, 3552-3555.
25. Wang, Q.; Ito, S.; Grätzel, M.; Fabregat-Santiago, F.; Mora-Serü, I.; Bisquert, J.; Bessho, T.; Imai, H. *J. Phys. Chem. B* **2006**, *110*(50), 25210-25221.
26. Adachi, M.; Sakamoto, M.; Jiu, J.; Ogata, Y.; Isoda, S. *J. Phys. Chem. B* **2006**, *110*, 13872-13880.